Contents lists available at ScienceDirect

Colloids and Surfaces A: Physicochemical and Engineering Aspects

journal homepage: www.elsevier.com

Surface properties of xylan and xylan derivatives measured by inverse gas chromatography

Sónia Sousa [a], Jorge Pedrosa [b], Ana Ramos [a], Paulo J. Ferreira [b], José A.F. Gamelas [b,*]

[a] FibEnTech and Department of Chemistry, University of Beira Interior, 6201-001 Covilhã, Portugal
[b] Department of Chemical Engineering, CIEPQPF, University of Coimbra, Pólo II − R. Silvio Lima, 3030-790 Coimbra, Portugal

ARTICLE INFO

Article history:
Received 9 May 2016
Received in revised form 1 July 2016
Accepted 3 July 2016
Available online xxx

Keywords:
Inverse gas chromatography
Wood xylan
Xylan derivatives
Surface energy
Lewis acid-base character

ABSTRACT

Xylan (the most common hemicellulose in wood and annual plants) and xylan derivatives have a very wide field of uses for which physico-chemical surface properties play an important role (e.g. in composites or barrier materials). In the present work, for the first time, inverse gas chromatography (at infinite dilution conditions) was used to assess the surface properties of xylan and xylan derivatives. Firstly, carboxymethyl xylan (CMX) and hydroxypropyl xylan (HPX) have been synthesized from commercial xylan (BX) and the presence of substituent groups confirmed by infrared spectroscopy and ^{1}H NMR. Then, the modified and original xylans were analysed for their dispersive component of the surface energy (γ_s^d) and Lewis acid-base properties. It was found that carboxymethylation and hydroxypropylation decreased significantly the γ_s^d value of xylan: from 47.6 mJ m^{-2} in BX to 33.0 mJ m^{-2} and 23.5 mJ m^{-2} in CMX and HPX, respectively. As for the Lewis acid-base properties, HPX showed a perfectly amphoteric behaviour while the surfaces of unmodified xylan and CMX showed a prevalence of Lewis acidic character over the Lewis basic character, being, however, the surface of CMX less acidic than that of the original xylan. These results were interpreted in terms of the effect of the presence of the new substituent groups in the xylan backbone.

1. Introduction

Hemicelluloses are the second most abundant natural polymer after cellulose, comprising about 25–35% of most plant materials, forest and agricultural residues [1–3]. Xylans are the most common hemicellulose in wood, as well in annual plants such as grasses, cereals, and herbs [4], representing about 10–35 wt% in hardwoods (e.g. eucalyptus, maple, birch) and 10–15 wt% in softwoods (e.g. spruce, pine and cedar) [5]. This polysaccharide is formed by β-(1 → 4)-linked D-xylopyranose (D-Xyl*p*) monomer units, being, however, the chemical structure dependent on the xylan source [6]. The main xylan in hardwood species is *O*-acetyl-4-*O*-methylglucuronoxylan while in softwood species is arabino-4-*O*-methylglucuronoxylan. The former is constituted by a main chain of D-Xyl*p* units with a few 4-*O*-methylglucuronic acid (MeGlcA) groups attached to the C-2 position of the xylan backbone and several hydroxyl groups substituted by acetyl groups at the C-2 and/or C-3 positions (about one MeGlcA group per 10–23 xylose units and 4–7 acetyl groups per 10 xylose units) [7–9]. The latter is a non-acetylated xylan where D-Xyl*p* units are branched with MeGlcA groups and α-L-arabinofuranose units [7].

Xylans have a very wide field of uses and their potential can be enhanced by chemical derivatization. They have been applied in the production of bioethanol, xylitol and *xylo*-oligosaccharides [3,6,10,11], as well as in films with low oxygen permeability [12–14], composites [15,16], hydrogels [17], surfactants [18], as paper additives and flocculation aids [19,20], antimicrobial agents [20] and coating color components [21]. In particular, they play an important role in pulping and papermaking processes as they increase the yield of the pulping process and improve the paper mechanical properties. However, the recent increasing demand for α-cellulose (dissolving pulp) and the production of nanocellulose open new possibilities for hemicelluloses production [21]. Moreover, the increasing demand for advanced renewable materials and green technologies has led researchers to focus their work in the plant biomass and value-added chemicals obtained from that. Abundant natural-based polymers, such as cellulose and hemicelluloses are, thus, of obviously high interest for both the scientific researchers as well as for the industry partners.

In this context, surface properties of xylans and modified xylans are an important parameter to consider in order to: (a) determine the influence of added functional groups in xylan's modification; (b) predict and optimize their compatibility with other polymers in the composites production; (c) expand their use in films for packaging and barrier materials. Inverse gas chromatography (IGC) is an appropriate tool to assess the surface properties of powdered solid materials, such as xylans, not possible to assess adequately, for instance, by classical contact-angle measurements (due to associated problems like porosity, roughness, surface heterogeneity). IGC enables to obtain the dispersive component of the surface energy, specific interactions (non-dispersive) with polar probes, Lewis acid-base character of the surface, surface nanoroughness parameter, Flory-Huggins interaction parameter [22–25], among other properties. This technique has been widely used for the study of cellulose and lignocellulosic materials

* Corresponding author.
Email address: jafgas@eq.uc.pt (J.A.F. Gamelas)

http://dx.doi.org/10.1016/j.colsurfa.2016.07.006
0927-7757/

[22] but, to our knowledge, it has never been reported before for the study of xylans of any type.

In the present work, a commercial beechwood xylan, and two modified xylans produced from commercial xylan by carboxymethylation and hydroxypropylation (Scheme 1) were analysed, for the first time, for their surface properties by inverse chromatography. Results of this study revealed significant differences between the several materials, namely for their dispersive component of the surface energy as well as for their Lewis acid-base properties.

2. Materials and methods

2.1. Materials

Beechwood xylan (BX) (Sigma-Aldrich, St. Louis, MO, USA) was used as the xylan source. Deuterium oxide (99.9 at.% D), (±)-propylene oxide (ReagentPlus 99%) and sodium monochloroacetate were purchased from Sigma-Aldrich (St. Louis, MO, USA). Sodium hydroxide (Pronalab, Lisbon, Portugal), hydrochloric acid, 2-propanol (Merck, Darmstadt, Germany), acetic acid, ethanol (Sigma-Aldrich, St. Louis, MO, USA), sulphuric acid (Panreac, Barcelona, Spain) and acetone (Scharlau, Barcelona, Spain), were used as reagent-grade chemicals. All probes for IGC analysis were of chromatographic grade and were used as received (Sigma–Aldrich, St. Louis, MO, USA).

2.2. Derivatizations of xylan

2.2.1. Carboxymethylation

Carboxymethyl xylan (CMX) synthesis was carried out according to a method reported by Petzold et al. [26]. Briefly, 5 g of BX (37.8 mmol of anhydro xylose units (AXU)) was dissolved in 25 mL of 25% aqueous sodium hydroxide solution followed by the addition of 35 mL of 2-propanol. The reaction mixture was stirred for 30 min at 30 °C. Then, 4.39 g (37.8 mmol) of sodium monochloroacetate was added and the temperature raised to 65 °C for 70 min. The reaction mixture was neutralized with diluted acetic acid, and then the CMX was precipitated and washed with ethanol, and finally dried at room temperature.

2.2.2. Hydroxypropylation

Hydroxypropyl xylan (HPX) synthesis was carried out according to the method used by Laine et al. [21]. Briefly, 13 g of 50% aqueous sodium hydroxide was added to 3.25 g of BX dispersed in distilled water (16.3%, w/w) was added and the mixture vigorously stirred in a pressure reactor. 7.6 mL of cooled propylene oxide was then added and the reaction mixture heated at 50 °C for 40 h. The reaction mixture was neutralized with 1 M hydrochloric acid solution, and then the HPX was precipitated by adding acetone. After washing, the HPX was freeze dried.

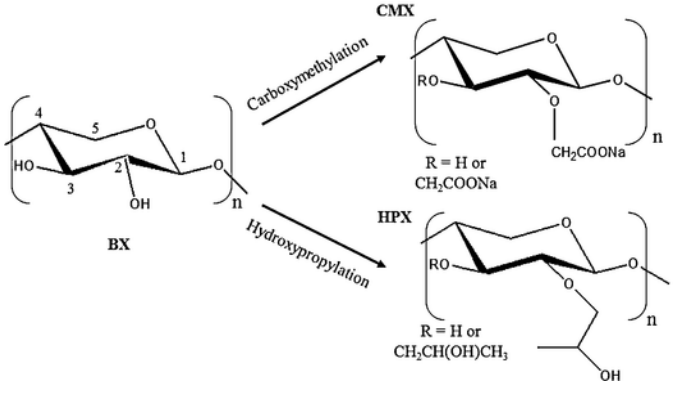

Scheme 1. Schematic representations of xylan, carboxymethyl xylan (CMX) and hydroxypropyl xylan (HPX) considered in the present study.

2.3. Characterization of xylans

2.3.1. Neutral sugar analysis

The determination of the neutral sugars composition of BX was undertaken after Saeman hydrolysis (treatment with 72% H_2SO_4 at 20 °C for 3 h, followed by 2.5 h hydrolysis with diluted 1 M H_2SO_4 at 100 °C). The released neutral monosaccharides were determined as alditol acetate derivatives by gas chromatography [27] using a Varian 3350 gas chromatograph equipped with a FID detector and a DB-225J&W column. The neutral sugars analysis of BX showed the predominance of xylose (97.1%) and the presence of small amounts of arabinose (1.2%), glucose (0.8%), rhamnose (0.4%), galactose (0.3%) and fucose (0.2%).

2.3.2. FTIR-ATR and ^{1}H NMR analyses

FTIR-ATR spectra were obtained using a Bruker Tensor 27 spectrometer and a MKII Golden Gate accessory with a diamond crystal 45° top plate. The spectra were recorded in the 500–4000 cm^{-1} range with a resolution of 4 cm^{-1} and a number of scans of 128.

^{1}H NMR spectra were collected in a Bruker Avance III 400 MHz NMR spectrometer with Bruker standard pulse program. Spectra of BX and CMX were acquired at room temperature while spectrum of HPX was also acquired at 5 °C (to shift the water signal overlapped with the H-1 signal). Samples, directly in the state of polymer chain, were dissolved in D_2O (10 mg mL^{-1}) for the acquisition of the ^{1}H NMR spectra. Sodium 3-(trimethylsilyl)propionate-*d4* (TMSP, δ 0.00) was used as internal standard.

The degree of substitution (DS) of the derivatized xylans was determined based on the NMR data. Note that, in each case, the modification should occur at the C-2 and C-3 positions of the xylan backbone. For CMX [28]: $DS = I_{H\text{-}1(s)}/(I_{H\text{-}1(u)} + I_{H\text{-}1(s)} + I_{H\text{-}1*})$, where $I_{H\text{-}1(s)}$ is the integrated area of fitted H-1 signals, at 4.59 ppm and *ca*. 4.53 ppm, of substituted AXU units at C-2 and C-3 positions, $I_{H\text{-}1(u)}$ is the integrated area of fitted H-1 signal at 4.49 ppm, of unsubstituted AXU units, and $I_{H\text{-}1*}$ is the integrated area of fitted H-1 signal at 4.63 ppm, of AXU units containing MeGlcA groups at C-2 position. For HPX [21]: $DS = (I_{methylprotons}/3)/I_{H\text{-}1}$, where $I_{methylprotons}$ is the integrated area of the signal due to three methyl protons in the hydroxypropyl group (peak at 1.13 ppm) and $I_{H\text{-}1}$ is the integrated area of the H-1 signal.

2.3.3. Inverse gas chromatography

The inverse gas chromatography analysis was performed using a DANI GC 1000 digital pressure control gas chromatograph equipped with a hydrogen flame ionization detector. Stainless-steel columns, 0.5 m long and 0.4 cm inside diameter were washed with acetone and dried before packing. After the packing of the material into the gas chromatograph column, the column was shaped in a smooth "U" to fit the detector/injector geometry of the instrument. The packed columns were conditioned overnight at 70 °C, under a helium flow (P = 0.05 bar), before any measurements were made. Measurements were carried out at four different temperatures (40, 45, 50 and 55 °C) for BX and CMX. For HPX, measurements were performed at the column temperature of 35 °C because only at this temperature (or lower) it was possible to obtain an acceptable separation between the retention times of the different probes (for a temperature of 40 °C

they were still very close to each other). The injector and detector were kept at 180 °C and 200 °C, respectively, and helium was used as carrier gas. Small quantities of probe vapour (<1 μL) were injected into the carrier gas, allowing work under infinite dilution conditions. The probes used for the IGC data collection were *n*-pentane (C5), *n*-hexane (C6), *n*-heptane (C7), *n*-octane (C8), *n*-nonane (C9), *n*-decane (C10), trichloromethane (TCM, Lewis acidic probe), dichloromethane (DCM, Lewis acidic probe), tetrahydrofurane (THF, Lewis basic probe), ethyl acetate (ETA, amphoteric) and acetone (amphoteric). The properties of the probes, of relevance to the IGC analysis, are listed in Table 1. It should be noted that, with the exception of DCM, polar probes with similar molecular surface area values and different electron donating/acceptor properties were chosen, in order to assess only the effect of Lewis acid-base interactions with the materials surface. DCM, an acidic probe with a lower molecular surface area, was useful to check the trend of the Lewis basic character between samples revealed by TCM. Methane was used as the reference probe. The retention times were the average of three injections and were determined by the Conder and Young method [30]. The coefficient of variation between runs was typically lower than 2%.

The theoretical aspects of inverse gas chromatography can be found elsewhere [22,24,25]. Briefly, the retention of a gas or vapour probe molecule in the IGC column is quantified by the net retention volume, V_n, which can be calculated from IGC data using Eq. (1), where t_r is the retention time of the injected probe through the column, t_0 is the retention time of the non-interacting probe (methane), F is the corrected flow rate of the inert carrier gas and J is the James–Martin correction factor for the carrier gas compressibility.

$$V_n = (t_r - t_o) \times F \times J \quad (1)$$

At infinite dilution conditions, the free energy of adsorption of the probe on the stationary phase surface (per mole), ΔG_a, can be determined from the retention volume, V_n, according to Eq. (2). In this equation, R is the gas constant and T is the column absolute temperature. The constant K is dependent on the chosen reference state [24].

$$\Delta G_a = -RT\ln(V_n) + K \quad (2)$$

If only dispersive interactions occur between sample and probe, the net retention volume, V_n, can be related to the dispersive components of the surface free energy of the interacting solid and probe, γ_s^d and γ_l^d, respectively, by Eq. (3), where N is the Avogadro number and a is the molecular surface area of the probe. According to Eq. (3), the dispersive component of the surface energy of the analysed sample may be estimated from the slope of the linear fit of $RT\ln(V_n)$ as a function of $2N \times a(\gamma_l^d)^{0.5}$, using the IGC data obtained with the apolar probes (Schultz and Lavielle approach [31]).

$$RT\ln(V_n) = \sqrt{\gamma_s^d}2N \times a\sqrt{\gamma_l^d} + K \quad (3)$$

For the polar probes, there is a corresponding specific component contribution, ΔG_a^s, in addition to the dispersive component, to the overall free energy of adsorption [24]. This parameter (ΔG_a^s) can be estimated by calculating the difference between the experimental value of $RT\ln(V_n)$ obtained for the polar probe and the corresponding estimation for the equivalent apolar probe (Eq. (4)) based on the linear fitting of $RT\ln(V_n)$ *vs*. $2N \times a(\gamma_l^d)^{0.5}$ for *n*-alkanes (reference line).

$$\Delta G_a^s = -RT\ln\frac{V_n}{V_{n,ref}} \quad (4)$$

The work of adhesion (W_a) can be obtained from the ΔG_a parameter, according to Eq. (5).

$$-\Delta G_a = N \times a \times W_a \quad (5)$$

Thus, using the inverse gas chromatography technique, the dispersive component of the surface energy (γ_s^d) and the specific components of the work of adhesion (W_a^s) of polar probes on the surface of the analysed materials were obtained.

Table 1
Properties of the probes used in the calculation of surface parameters by IGC[a].

Probe	Type	a (Å^2)	γ_l^d (mJ m^{-2})	DN (KJ mol^{-1})	AN* (KJ mol^{-1})
n-pentane	apolar	46.1	16.0		
n-hexane	apolar	51.5	18.4		
n-heptane	apolar	57.0	20.3		
n-octane	apolar	63.0	21.3		
n-nonane	apolar	69.0	22.7		
n-decane	apolar	75.0	23.4		
trichloromethane	acid	44.0	25.0	0	22.7
dichloromethane	acid	31.5	27.6	0	16.4
tetrahydrofurane	base	45.0	22.5	84.4	2.1
ethyl acetate	amphoteric	48.0	19.6	71.8	6.3
acetone	amphoteric	42.5	16.5	71.4	10.5

[a] Data taken from references [22,25,29]. a is the molecular surface area of the probe, γ_l^d is the dispersive component of the surface energy of the probe, DN and AN* are the Gutmann's electron donor and electron acceptor numbers, respectively, of the acid-base probe.

3. Results and discussion

3.1. Chemical characterization of xylan and xylan derivatives

The produced xylan derivatives (and the original xylan for comparison) were firstly characterized by infrared spectroscopy and ^{1}H NMR to confirm the presence of the substituent groups and determine the corresponding degree of substitution. The FTIR spectrum of BX (Fig. 1) showed the characteristic polysaccharide bands, namely: a sharp band at 897 cm^{-1} due to C1—H bending mode, which is characteristic of β-glycosidic linkages between the sugar units [32]; several bands between 1500 and 1000 cm^{-1} due to the C—H bending

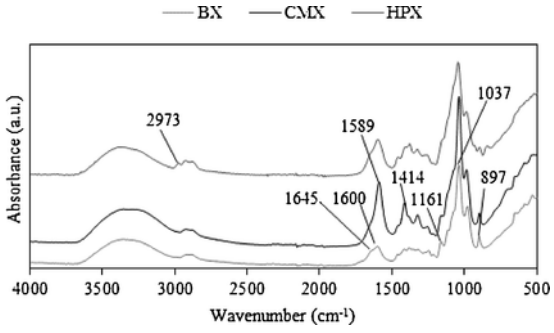

Fig. 1. FTIR-ATR spectra of beechwood xylan (BX), carboxymethyl xylan (CMX) and hydroxypropyl xylan (HPX).

and C—O stretching vibrations, with an absorption maximum at 1037 cm^{-1} and a band at 1161 cm^{-1} due to the asymmetric stretching of C—O—C glycosidic bonds [32]; bands due to the C—H stretching between 2870 and 2920 cm^{-1}; and a broad band at ca. 3400 cm^{-1} due to hydroxyl bond stretching [33,34]. In the 1500–1700 cm^{-1} region, bands at 1600 cm^{-1} and ca. 1645 cm^{-1} (shoulder) from ionized glucuronic acid groups and sorbed water, respectively, were also observed [33–35]. For CMX (Fig. 1) as compared to BX, an additional strong band at 1589 cm^{-1} ascribed to the asymmetric stretching of the COO^- groups in the carboxymethyl xylan [36] appeared in the FTIR spectrum, showing successful carboxymethylation. The band at 1414 cm^{-1}, assigned to the CH_2 bending, was also enhanced in intensity, as the result of the substitution of O—H by O—CH_2COO^- groups in the xylan backbone. The FTIR spectrum of the obtained CMX also resembles that of a commercial sample of carboxymethylcellulose (results not shown). Finally, in the HPX spectrum (Fig. 1), an additional band at 2973 cm^{-1}, assigned to the asymmetric C—H stretching of the methyl groups from the hydroxypropyl moieties [37] was observed, providing thereby the evidence that hydroxypropylation has occurred.

The ^{1}H NMR spectrum of BX (Fig. 2) showed major signals corresponding to AXU at 4.49 ppm (H-1, anomeric), 3.29 ppm (H-2), 3.56 ppm (H-3), 3.80 ppm (H-4), 3.38 ppm (H-5_{ax}) and 4.10 ppm (H-5_{eq}). Additionally, the presence of 4-*O*-methylglucuronic acid (MeGlcA) was detected by the signals at 5.29 and 3.47 ppm corresponding to H-1 and methoxy protons, respectively [8,38,39]. The ratio between the peak areas of the anomeric protons of MeGlcA and AXU indicates that one MeGlcA group is present per 10 AXU. In the spectrum of CMX (Fig. 2), close to the signal of the anomeric proton at 4.49 ppm, less intense signals appeared at ca. 4.53 and 4.59 ppm. The latter can be attributed to H-1 of functionalized units in *O-3*/*O-2* positions of AXU [28]. From the comparison of the integrated area of these signals and that of H-1 of unsubstituted units, a DS of 0.30 was calculated (as explained in previous Section 2.3.2) for CMX. The ^{1}H NMR spectrum of HPX (Fig. 2) showed a very intense signal at 1.13 ppm clearly attributed to the methyl protons of the substituent hydroxypropyl groups [21]. From the comparison of the integrated area of this signal and that of anomeric H-1, a DS of 1.07 was determined for HPX (Section 2.3.2). Overall, infrared spectroscopy and ^{1}H NMR revealed that successful derivatizations of BX have been achieved. The degree of substitution was of 0.3 for CMX and 1.1 for HPX.

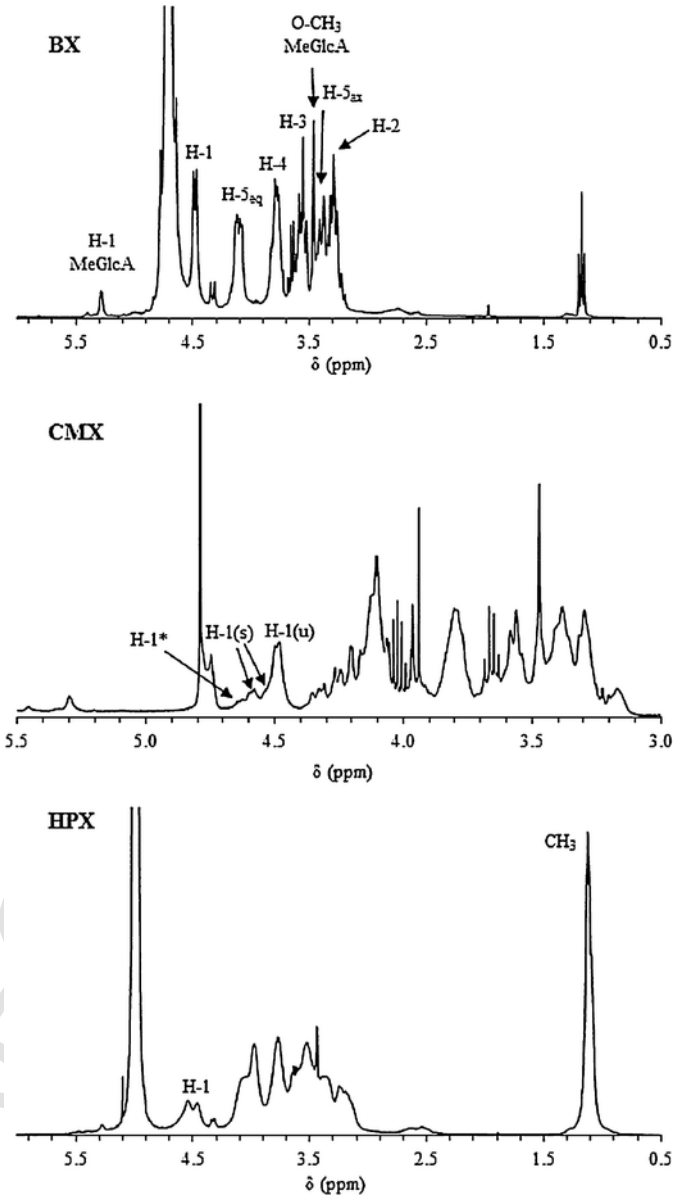

Fig. 2. ^{1}H NMR spectra of beechwood xylan (BX), carboxymethyl xylan (CMX) and hydroxypropyl xylan (HPX) in D_2O (spectrum of hydroxypropyl xylan at 5 °C and the others at room temperature). "u" and "s" denote unsubstituted and substituted AXU units, respectively, and "*" denotes AXU units containing MeGlcA groups.

3.2. Surface properties assessed by inverse gas chromatography

The dispersive component of the surface energy was determined from the plots of $RT\ln(V_n)$ as a function of $2N \times a \times (\gamma_l^d)^{0.5}$ (Schultz and Lavielle approach, Fig. 3). The results are presented in Table 2. The γ_s^d (at 40 °C, and at 35 °C for HPX) varied in the following order: BX > CMX > HPX. The relatively high value of γ_s^d observed for unmodified xylan can be majorly related to a higher amount/accessibility of hydroxyl groups (which are able to establish dispersive interactions with the *n*-alkanes [35,40]) on the surface of this xylan. No previous studies of xylans surfaces by IGC were found in the literature; however, the γ_s^d value here obtained for beech xylan is in the same range of those reported for other polysaccharides such as cellulose and bleached pulps (40–50 mJ m^{-2} range) [22]. On the other hand, the substitution of hydrogen atoms from hydroxyls by carboxymethyl groups in the carboxymethyl xylan or by hydroxypropyl groups in the hydroxypropyl xylan decreased significantly the γ_s^d value probably because the new attached groups are less able/accessible for dispersive interactions than the hydroxyl groups. This effect was more pronounced in the hydroxypropyl xylan being obtained a γ_s^d value as low as 23.5 mJ m^{-2}, that indicates a low surface energy material. A value of similar magnitude (25 mJ m^{-2}, at 40 °C) was obtained for hydroxypropylcellulose [41]. Note, however, that the straight comparison of CMX with HPX should be made with due care, since these modified xylans were obtained with a different degree of substitution. For a CMX with a higher DS, a lower γ_s^d value, closer to that of HPX, could be obtained.

Additionally, the effect of temperature on the γ_s^d parameter was also studied. For the unmodified xylan a decreasing trend of the γ_s^d value with temperature in the range of studied temperatures (40–55 °C) was found (Fig. 4), as previously observed for related cellulosic materials [35,42]. For the CMX the variation of the γ_s^d value

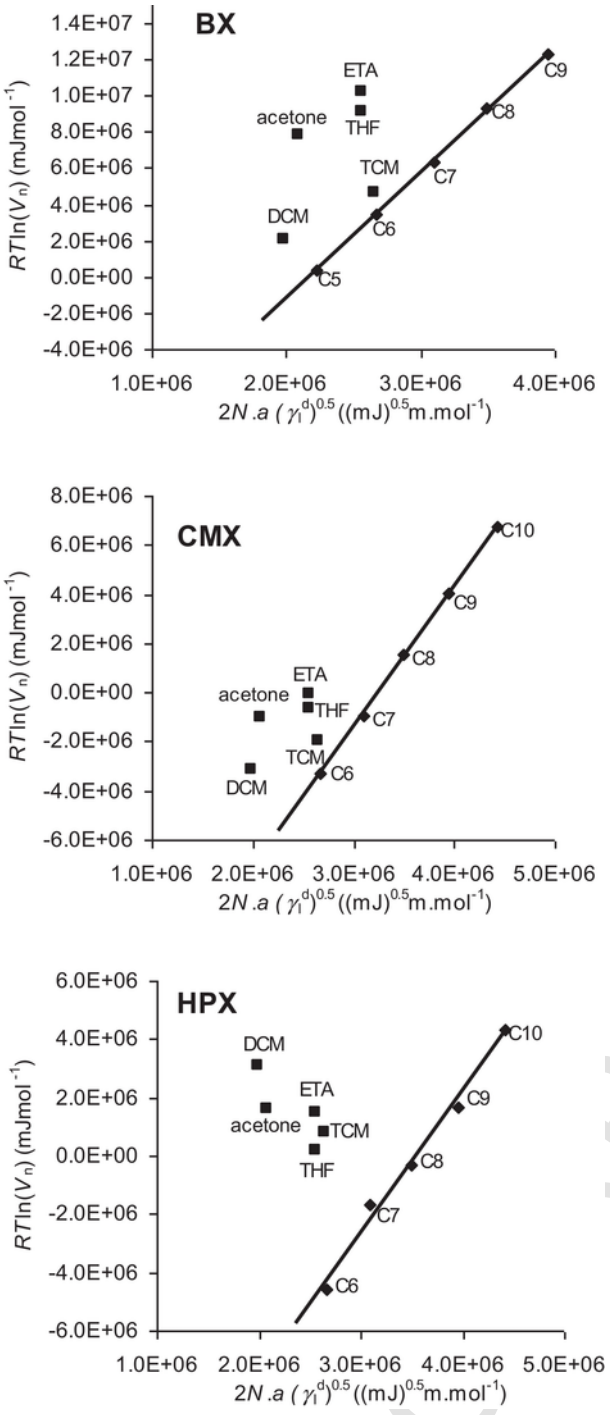

Fig. 3. Plots of $RT\ln(V_n)$ vs. $2N \times a(\gamma_l^d)^{0.5}$ for beechwood xylan (BX), carboxymethyl xylan (CMX) and hydroxypropyl xylan (HPX). Results at 40 °C, and at 35 °C for HPX.

with temperature (in the same temperature range) was somewhat different: it decreased from 40 to 45 °C and then reached a plateau (Fig. 4). These results show, thus, a different behaviour of CMX in comparison to BX as a consequence of the chemical modification. As mentioned before (Section 2.3.3), for HPX it was not possible to study the effect of temperature increase because the retention times of the different tested probes were all very close to each other at temperatures ≥40 °C, precluding the determination of any IGC surface parameters.

The Lewis acid–base character of the xylans surface was assessed based on the calculation of the specific component of the work of adhesion (W_a^s) of different polar probes (Schultz and Lavielle approach, Fig. 3). The results shown in Table 2 for the different probes (excluding DCM) indicate that: (a) the xylans are amphoteric since they all present higher affinity with Lewis amphoteric probes (acetone, ETA) and; (b) the original xylan and CMX have more Lewis acidic than basic character since the affinity with basic (THF) probe is higher than with acidic (TCM) probe; and (c) HPX was a perfectly amphoteric material because specific affinity of Lewis acidic probe (TCM) and of basic one (THF) were very similar. The acidic surface character of xylans is attributed to the dominant presence of acidic hydroxyl (and carboxylic acid) groups. On the other hand, oxygen's in oxygen-carbon linkages and carboxymethyl groups are expected to have a more Lewis basic than Lewis acidic character and thus to contribute more to the Lewis basicity of the material surface. Note that for the same sample, the specific interaction of DCM should not be compared to those of the other probes in terms of assessing only the Lewis acid-base character of the material surface, because DCM has a significantly lower molecular surface area (Table 1). In fact, although DCM and TCM have comparable electron acceptor properties (Table 1) significantly higher specific interactions are always obtained for the former (Table 2) because DCM molecules are less bulky, thus being less likely to steric constraints in the interaction with the material surface. However, DCM may be used, when comparing the different samples, to corroborate the results obtained with TCM, as follows below.

The specific interactions at temperatures higher than 40 °C were also obtained for the unmodified xylan and CMX. For the original xylan, the W_a^s values of each probe were similar in the 40–55 °C range (see Fig. 5 for the results at 40 and 50 °C). However, for CMX some differences were found between the specific components values obtained at 40 °C and at higher temperatures. In fact, a significant increase of the W_a^s values was noted, particularly those of Lewis acidic probes, when increasing temperature from 40 °C to 45–50 °C (Fig. 5). Further studies to clarify the behaviour of CMX with temperature will certainly have to be done.

The results of the specific interactions of beech xylan are not far from those previously reported for e.g., cellulosic materials [22]. Due to the substitution of acidic hydroxyls by Lewis basic groups in CMX, the affinity with basic and amphoteric probes (THF, ETA and acetone) greatly decreased accompanied by an increase of the affinity to Lewis acidic probes (TCM and DCM) (Table 2). The overall result was a significant decrease of the W_a^s(THF)/W_a^s(TCM) ratio. Note, again, that the present CMX was obtained with a relatively low DS. For higher DS values, lower W_a^s(THF)/W_a^s(TCM) ratios may be expected. The HPX showed a perfectly amphoteric behaviour, with a W_a^s(THF)/W_a^s(TCM) ratio close to 1. Here, the specific interactions with basic THF and amphoteric ETA probe were lower than those observed for beech xylan, while the specific interaction with acetone was close to that obtained for beech xylan. Interestingly, the specific interactions with acidic probes (both TCM and DCM) were considerably higher than those obtained for the other xylans. The substitution in xylan of hydroxyls (—OH), that are mostly acidic in character, by —O—CH_2—CH(OH)CH_3 groups that possess both Lewis basic and acidic sites, will confer the observed amphoteric character to the material surface, including the decrease of the Lewis acidity and the increase of the Lewis basicity. Determinations of the specific component of the enthalpy of adsorption (ΔH_a^s) for the same probes on hydroxypropyl cellulose also revealed a material with an amphoteric behaviour [41].

Table 2
Dispersive component of the surface energy (γ_s^d, mJ m^{-2}) and specific component of the work of adhesion (W_a^s, mJ m^{-2}) of polar probes for beech xylan and modified xylans[a].

Material	γ_s^d	W_a^s (TCM)	W_a^s (DCM)	W_a^s (THF)	W_a^s (ETA)	W_a^s (acetone)	W_a^s(THF)/W_a^s(TCM)
BX	47.6	5.0	17.5	23.5	25.9	33.0	4.7
CMX	33.0	5.3	21.5	11.9	13.4	22.0	2.3
HPX	23.5	19.5	56.1	18.3	21.7	33.9	0.94

[a] Values at 40 °C (and 35 °C for HPX) calculated following Schultz and Lavielle approach [31].

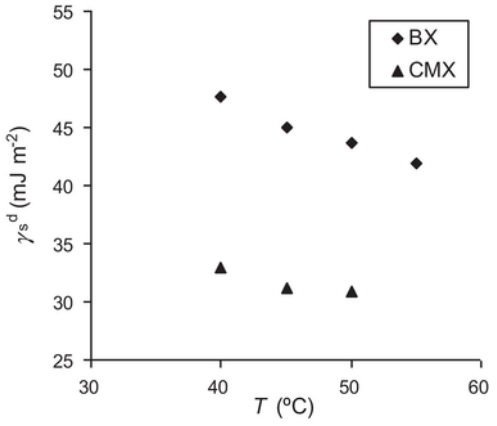

Fig. 4. γ_s^d values at several temperatures for beechwood xylan (BX) and carboxymethyl xylan (CMX) (the result of CMX at 55 °C is not shown because of poor linear fitting).

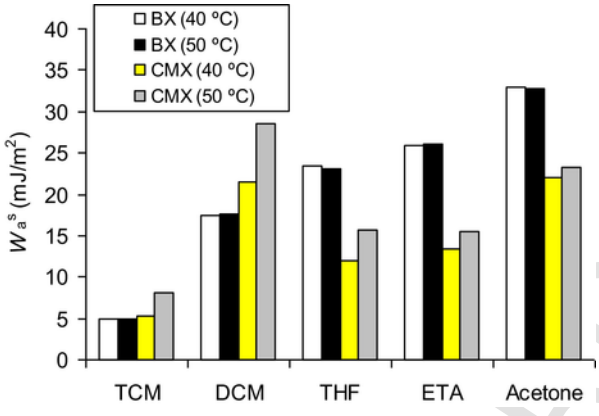

Fig. 5. Specific component of the work of adhesion (W_a^s) of several Lewis acid-base probes on the surface of beechwood xylan (BX) and carboxymethyl xylan (CMX) at 40 and 55 °C.

4. Conclusions

A commercial beechwood xylan was carboxymethylated and hydroxypropylated to degrees of substitution of 0.3 and 1.1, respectively. Results from IGC analysis revealed that the dispersive component of the surface energy of the beechwood xylan is reasonably high (47.6 mJ m^{-2}) and that the introduction of carboxymethyl and hydroxypropyl groups significantly decreases this component. This effect was more pronounced for hydroxypropyl xylan where a γ_s^d value as low as 23.5 mJ m^{-2} was obtained. The higher extent of modification achieved for this xylan derivative could also be responsible for the lower value obtained for γ_s^d. The W_a^s(THF)/W_a^s(TCM) ratio, that measures the prevalence of the Lewis acidity over the Lewis basicity of the material surface, was of 4.7 for BX, 2.3 for CMX and 0.94 for HPX. Thus, as a consequence of the substitution of a few hydroxyl acidic groups by carboxymethyl basic groups in CMX, the surface of CMX possessed less acidic character than that of BX. As for HPX, with a high substitution degree, the results revealed an amphoteric nature of —O—CH_2—CH(OH)CH_3 groups. The injection of other Lewis acidic and amphoteric probes confirmed these trends.

Acknowledgements

This work was carried out in the framework of the FCOMP-01-0202-FEDER-011500 (NMC) project.

References

[1] N. Mosier, C. Wyman, B. Dale, R. Elander, Y. Lee, M. Holtzapple, M. Ladisch, Features of promising technologies for pretreatment of lignocellulosic biomass, Bioresour. Technol. 96 (2005) 673–686.
[2] B. Saha, Hemicellulose bioconversion, J. Ind. Microbiol. Biotechnol. 30 (2003) 279–291.
[3] Y. Sun, J. Cheng, Hydrolysis of lignocellulosic materials for ethanol production: a review, Bioresour. Technol. 83 (2002) 1–11.
[4] A. Ebringerová, T. Heinze, Xylan and xylan derivatives—biopolymers with valuable properties, 1. Naturally occurring xylans structures, isolation procedures and properties, Macromol. Rapid Commun. 21 (9) (2000) 542–556.
[5] K. Hettrich, S. Fischer, N. Schroder, J. Engelhardt, U. Drechsler, F. Loth, Derivatization and characterization of xylan from oat spelts, Macromol. Symp. 232 (2006) 37–48.
[6] R. Deutschmann, R.F.H. Dekker, From plant biomass to bio-based chemicals: latest developments in xylan research, Biotechnol. Adv. 30 (6) (2012) 1627–1640.
[7] M.P. Coughlan, G.P. Hazlewood, Beta-1,4-D-xylan-degrading enzyme systems: biochemistry, molecular biology and applications, Biotechnol. Appl. Biochem. 17 (1993) 259–289.
[8] D.V. Evtuguin, J.L. Tomás, A.M.S. Silva, C.P. Neto, Characterization of an acetylated heteroxylan from Eucalyptus globulus Labill, Carbohydr. Res. 338 (2003) 597–604.
[9] A. Teleman, M. Tenkanen, A. Jacobs, O. Dahlman, Characterization of O-acetyl-(4-O-methylglucurono)xylan isolated from birch and beech, Carbohydr. Res. 337 (2001) 373–377.
[10] X. Chen, Z.-H. Jiang, S. Chen, W. Qin, Microbial and bioconversion production of D-xylitol and its detection and application, Int. J. Biol. Sci. 6 (7) (2010) 834–844.
[11] A. Reis, P. Pinto, D.V. Evtuguin, C.P. Neto, P. Domingues, A.J. Ferrer-Correia, R.M. Domingues, Electrospray tandem mass spectrometry of underivatised acetylated xylo-oligosaccharides, Rapid Commun. Mass Spectrom. 19 (2005) 3589–3599.
[12] M. Gröndahl, L. Eriksson, P. Gatenholm, Material Properties of plasticized hardwood xylans for potential application as oxygen barrier films, Biomacromolecules 5 (2004) 1528–1535.
[13] J. Hartman, A.-C. Albertsson, M.S. Lindblad, J. Sjöberg, Oxygen barrier materials from renewable sources: materials properties of softwood hemicellulose-based films, J. Appl. Polym. Sci. 100 (2006) 298.
[14] N.M.L. Hansen, D. Plackett, Sustainable films and coatings from hemicelluloses: a review, Biomacromolecules 9 (6) (2008) 1494–1505.
[15] X.-w. Peng, J.-l. Ren, L.-x. Zhong, R.-c. Sun, Nanocomposite films based on xylan-rich hemicelluloses and cellulose nanofibers with enhanced mechanical properties, Biomacromolecules 12 (2011) 3321–3329.
[16] A. Saxena, T.J. Elder, S. Pan, A.J. Ragauskas, Novel nanocellulosic xylan composite films, Compos. Part B Eng. 40 (2009) 727–730.
[17] H. Pohjanlehto, H. Setälä, K. Kammiovirta, A. Harlin, The use of N,N′-diallyladardiamides as cross-linkers in xylan derivatives-based hydrogels, Carbohydr. Res. 346 (2011) 2736–2745.
[18] F. Bouxin, S. Marinkovic, J. Le Bras, B. Estrine, Direct conversion of xylan into alkyl pentosides, Carbohydr. Res. 345 (17) (2010) 2469–2473.

[19] J. Kataja-aho, S. Haavisto, J. Asikainen, S. Hyvärinen, S. Vuoti, The influence of cationized birch xylan on wet and dry strength of fine paper, Bioresources 7 (2) (2011) 1713–1728.
[20] K. Petzold-Welcke, K. Schwikal, S. Daus, T. Heinze, Xylan derivatives and their application potential—mini-review of own results, Carbohydr. Polym. 100 (2014) 80–88.
[21] C. Laine, A. Harlin, J. Hartman, S. Hyvärinen, K. Kammiovirta, B. Krogerus, H. Pajari, H. Rautkoski, H. Setälä, J. Sievänen, J. Uotila, M. Vähä-Nissi, Hydroxyalkylated xylans—their synthesis and application in coatings for packaging and paper, Ind. Crop. Prod. 44 (2013) 692–704.
[22] J.A.F. Gamelas, The surface properties of cellulose and lignocellulosic materials assessed by inverse gas chromatography: a review, Cellulose 20 (2013) 2675–2693.
[23] J.A.F. Gamelas, E. Ferraz, F. Rocha, An insight into the surface properties of calcined kaolinitic clays: the grinding effect, Colloids Surf. A 455 (2014) 49–57.
[24] P. Mukhopadhyay, H.P. Schreiber, Aspects of acid-base interactions and use of inverse gas chromatography, Colloids Surf. A 100 (1995) 47–71.
[25] J.M.R.C.A. Santos, J.T. Guthrie, Analysis of interactions in multicomponent polymeric systems: the key-role of inverse gas chromatography, Mat. Sci. Eng. R. 50 (2005) 79–107.
[26] K. Petzold, K. Schwikal, T. Heinze, Carboxymethyl xylan—synthesis and detailed structure characterization, Carbohydr. Polym. 64 (2006) 292–298.
[27] R.R. Selvedran, J.F. March, S.G. Ring, Determination of aldoses and uronic acids content of vegetable fiber, Anal. Biochem. 96 (1979) 282–292.
[28] I. Šimkovic, I. Kelnar, I. Uhliariková, R. Mendichi, A. Mandalika, T. Elder, Carboxymethylated-, hydroxypropylsulfonated- and quaternized xylan derivative films, Carbohydr. Polym. 110 (2014) 464–471.
[29] D.P. Kamdem, S.K. Bose, P. Luner, Inverse gas chromatography characterization of birch wood meal, Langmuir 9 (1993) 3039–3044.
[30] D.P. Kamdem, B. Riedl, Inverse gas chromatography of lignocellulosic fibers coated with a thermosetting polymer: use of peak maximum and conder and young methods, J. Colloid Interface Sci. 150 (1992) 507–516.
[31] J. Schultz, L. Lavielle, C. Martin, The role of the interface in carbon fibre-epoxy composites, J. Adhesion 23 (1987) 45–60.
[32] M. Kacurákova, P. Capek, V. Sasinkova, N. Wellner, A. Ebringerová, FTIR study of plant cell wall compounds: pectic polysaccharides and hemicelluloses, Carbohydr. Polym 43 (2000) 195–203.
[33] R.H. Marchessault, C.Y. Liang, The infrared spectra of crystalline polysaccharides. VIII. Xylans, J. Polym. Sci. A 59 (1962) 357–378.
[34] D.K. Buslov, F.N. Kaputski, N.I. Sushko, V.I. Torgashev, L.V. Solov'eva, V.M. Tsarenkov, O.V. Zubets, L.V. Larchenko, Infrared spectroscopic analysis of the structure of xylans, J. Appl. Spectr. 76 (2009) 801–805.
[35] J.A.F. Gamelas, J. Pedrosa, A.F. Lourenço, P.J. Ferreira, Surface properties of distinct nanofibrillated celluloses assessed by inverse gas chromatography, Colloids Surf. A 469 (2015) 36–41.
[36] J.-L. Ren, R.-C. Sun, F. Peng, Carboxymethylation of hemicelluloses isolated from sugarcane bagasse, Polym. Degrad. Stabil. 93 (2008) 786–793.
[37] V.K. Varshney, S. Naithani, Chemical functionalization of cellulose derived from nonconventional sources, in: S. Kalia, B.S. Kaith, I. Kaur (Eds.), Cellulose Fibers: Bio- and Nano-polymer Composites—Green Chemistry and Technology, 2011Springer, pp. 43–60.
[38] F.-Z. Belmokaddem, C. Pinel, P. Huber, M. Petit-Conil, D.S. Perez, Green synthesis of xylan hemicellulose esters, Carbohydr. Res. 346 (2011) 2896–2904.
[39] N.G.V. Fundador, Y. Enomoto-Rogers, A. Takemura, T. Iwata, Syntheses and characterization of xylan esters, Polymer 53 (2012) 3885–3893.
[40] G. Garnier, W.G. Glasser, Measuring the surface energies of spherical cellulose beads by inverse gas chromatography, Polym. Eng. Sci. 36 (1996) 885–894.
[41] B. Sasa, P. Odon, S. Stane, K. Julijana, Analysis of surface properties of cellulose ethers and drug release from their matrix tablets, Eur. J. Pharm. Sci. 27 (2006) 375–383.
[42] M.G. Carvalho, J.M.R.C.A. Santos, A.A. Martins, M.M. Figueiredo, The effects of beating, web forming and sizing on the surface energy of Eucalyptus globulus kraft fibres evaluated by inverse gas chromatography, Cellulose 12 (2005) 371–383.